3D Interdigitated Electrodes for Point-of-Care Electrochemical Biosensing

Benjamin J. Brownlee and Brian D. Iverson
Department of Mechanical Engineering
Brigham Young University

ABSTRACT

Increased sensor sensitivity is important for enabling detection of low concentrations of target analyte. Being able to quickly and accurately detect low concentrations of proteins at point-of-care allows for results to be analyzed more easily and effectively. Vertically-aligned carbon nanotubes (VACNTs) were patterned into interdigitated electrodes (IDEs) and then functionalized with the representative protein streptavidin that was functionalized on the VACNT surfaces by covalent bonding (with EDC/NHS). Further detection was observed by binding biotin to the streptavidin. Fluorescence microscopy enabled the optimization of protein loading on VACNTs. Cyclic voltammetry and electrochemical impedance spectroscopy were used to characterize the electrodes and monitor the associated changes with the addition of streptavidin and biotin. A unique change in impedance is observed, which allows for monitoring the quantity of target analyte bound to the VACNT electrode surface with an observed 14x increase in resistance.

INTRODUCTION

Point-of-care diagnostics has gained interest among researchers because it enables cost effective and rapid results that were typically done by ELISA in the past, a process that requires extensive equipment and expertise as well as much longer processing times. Development of electrochemical biosensors have pushed toward the ability diagnose at in-field point-of-care use. While other methods of detection have been used, such as optical methods, electrochemical sensors have the advantage of being repeatable, affordable, and easy to use [1]. In particular, electrochemical sensors that are in an interdigitated electrode (IDE, see Figure 1A) design exhibit low ohmic drops, high signal-to-noise ratios, and fast response times [2].

Carbon nanomaterials (carbon nanotubes, graphene, and graphene oxide), have been shown to be effective at increasing sensor sensitivity [3]. Specifically, microstructured surfaces, greatly increase electrode surface area and have been shown to outperform planar geometries [4]. Vertically-aligned carbon nanotubes (VACNTs) are an excellent example as they provide high surface area to volume ratio and are highly conductive, making VACNTs a useful electrochemical electrode nanomaterial.

VACNTs have previously been used in an IDE configuration for the detection of an oral cancer markers [5] and this work seeks to build upon and generalize the findings that work. VACNTs have also been used for detection of hydrogen peroxide (H_2O_2) with a flow-through VACNT electrode [6]. The three dimensional nature of the VACNT electrode, as schematically shown in Figure 1B, provides the advantage of having a large surface-area-to-volume ratio that enables higher protein capture capacity relative to planar electrodes, leading to improved sensitivity [7].

In the present work we have manufactured a VACNT IDE electrode (~ 30 µm tall) for impedance-based biosensing. The electrodes were functionalized by covalently binding the representative protein streptavidin on to the VACNT surfaces. Biotin was then bound to the streptavidin as an example of small molecule detection. Fluorescence microscopy enabled the optimization of protein loading on VACNTs. Cyclic voltammetry and electrochemical impedance spectroscopy were used to characterize the electrodes. Both electrochemical methods show a change with the addition of streptavidin and biotin, with a unique change in impedance which allows for detection of target analyte bound to the VACNT electrode surface.

MATERIALS AND METHODS

VACNT fabrication methods were similar to previously published protocols [6, 8]. Starting with a 100 mm oxidized silicon (Si) wafer with a 1 µm oxide layer, 50 nm of aluminum oxide (Al_2O_3) was deposited by electron beam evaporation. Photolithography was used to pattern positive photoresist (AZ3330) into interdigitated electrodes (IDEs) with 30 fingers per side, 25 µm finger width, 25 µm finger spacing, and 2 mm finger length (see Figure 1A for schematic representation of an IDE). A 7 nm film of iron (Fe) was thermally evaporated onto the patterned photoresist, followed by sonication in N-Methyl-2-pyrrolidone (NMP) for at least 10 minutes for lift-off patterning of Fe (see schematic of layers used in Figure 1C). The patterned wafer was diced into 16.1 x 8.0 mm rectangles using a diamond-coated blade.

VACNTs were grown by chemical vapor deposition (CVD) in a 1-inch diameter tube furnace with flowing hydrogen (H_2, 311 sccm) and ethylene
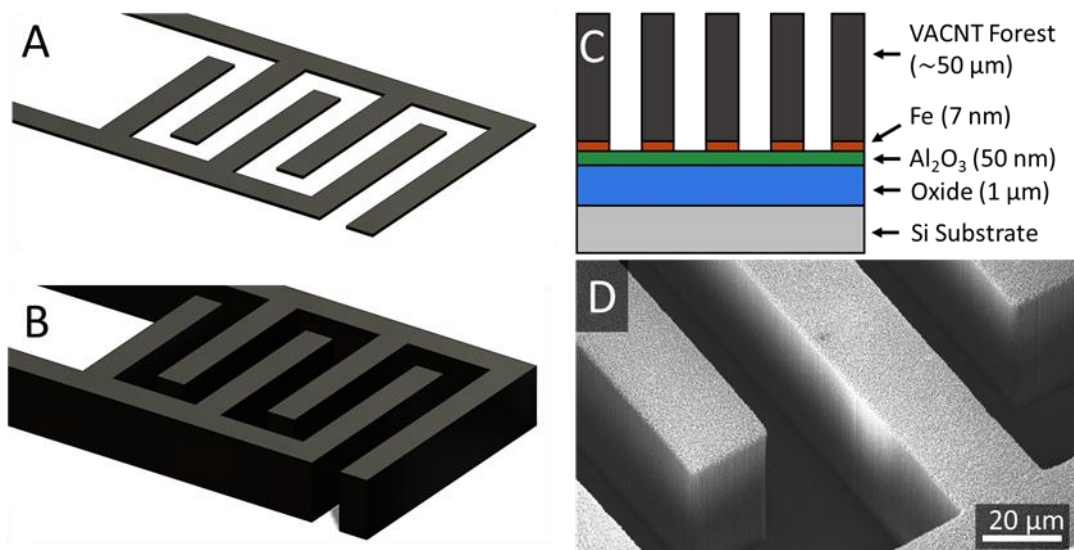
Figure 1. Schematic representation of (A) planar and (B) 3D interdigitated electrodes. (C) Schematic of layers used to manufacture the VACNT sensor architecture: Si, oxide, Al₂O₃, Fe, and VACNTs. (D) Scanning electron microscope (SEM) image of 3D VACNT electrodes.

(C_2H_4, 338 sccm) at 750 °C for 30 seconds. The temperature was then raised to 900 °C and the H_2 flow rate reduced to 190 sccm to infiltrate (coat) the VACNTs with amorphous carbon for 2 minutes (C_2H_4 flow rate was unchanged). This infiltration process strengthened the VACNT structure to create a sturdy, porous 3D IDE about 30 μm tall (see Figure 1D). The amorphous carbon not only coated the VACNTs, but also the substrate, creating an electrical short between the two electrodes. To remove the carbon on the substrate, the devices were placed in an oxygen plasma etch for 30 seconds in a Technics Planar Etch II machine (250 W, 300 mTorr).

Silver epoxy was manually applied to contact pads and part of the electrode leads to strengthen the contact when connected with alligator clips. This silver epoxy was then manually coated with an inert polish to prevent electrochemical interaction and to ensure consistent coverage of the electrode by the electrolyte with repeat tests.

Fluorescently marked Atto 425 Streptavidin (Sigma-Aldrich 09260), hereafter simply referred to as streptavidin, was covalently bonded to the VACNT IDE using 1-ethyl-3-(-3-dimethylaminopropyl) carbodiimide (EDC, Sigma-Aldrich E7750) and N-hydroxysuccinimide (NHS, Sigma-Aldrich 130672) chemistry. The VACNT electrode was incubated at room temperature in 50 μL of 100 mM EDC and 100 mM NHS in 0.1 M 2-(N-morpholino) ethanesulfonic acid (MES, pH 4.7, Thermo Scientific 28390). The electrode was then rinsed with ultrapure water and then incubated in 50 μL of 20, 100, or 500 μg/mL streptavidin in phosphate buffered saline (1X PBS, pH 7.4, Fisher Scientific) at room temperature for at least

16 hours (overnight). During the soaking, the electrode was placed in an air-tight container to prevent evaporation of the droplet. After the soaking, the electrode was again rinsed with ultrapure water.

Fluorescently tagged Atto 565 Biotin (Sigma-Aldrich 92637), hereafter simply referred to as biotin, binds with streptavidin in the strongest known non-covalent bond between a protein and a ligand. The streptavidin-coated VACNT electrode was incubated in 50 μL of 200 μg/mL biotin at room temperature for 60 minutes, after which it was thoroughly rinsed with ultrapure water. The biotin/streptavidin-coated VACNT electrode is represented in Figure 2, noting that up to 4 biotin molecules can bind with a single streptavidin protein.

Fluorescent microscopy was done with an Olympus FluoView FV1000 confocal laser scanning microscope. A wavelength of 405 nm was used to excite the fluorescent streptavidin and a wavelength of 543 nm was used to excite the fluorescent biotin. Fluorescent markers have very little overlap in absorption and emission so that the intensity of each is
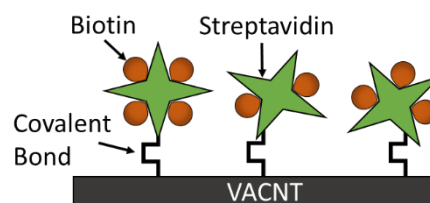

Figure 2. Schematic of functionalized VACNTs showing the larger streptavidin covalently bound to the VACNT surface and the smaller biotin bound with the streptavidin.

nearly independent of the presence of the other. Specific microscope settings included: 12% laser power, 800 HV, 6 offset, aperture at 200 μm and 20x magnification.

All electrochemical experiments were performed with a CH Instuments (CHI) 660E Potentiostat/ Galvanostat. For cyclic voltammetry experiments the following electrodes were used: a saturated (KCl) Ag/AgCl reference electrode, a platinum wire counter electrode, and one side of the VACNT electrode as the working electrode. For electrochemical impedance spectroscopy (EIS), one side of the IDE was the reference and counter electrode and the other side of the IDE was the working electrode.

Electrochemical experiments were performed in a 15 mL solution of 5 mM $K_3[Fe(CN)_6]$ (potassium ferricyanide), 5 mM $K_4[Fe(CN)_6]$ (potassium ferrocyanide) and 0.1 M KCl at room temperature and typical air exposure.

RESULTS AND DISCUSSION

VACNT heights (electrode thicknesses) were measured to be about 30 μm. With the spacing and width of the IDEs being 25 μm, the height-to-width ratio of the electrodes was about 1:1.

Because amorphous carbon was added to the VACNTs, there were plenty of site defects that provided carboxyl groups on the electrode surface. These carboxyl groups allowed for covalent bonding with the amine group on proteins through EDC/NHS chemistry. However, there are many different reported recipes for EDC/NHS chemistry. Some variables include single solution vs two-step solution, buffer solution, overall concentration, ratio of EDC to NHS, incubation time, and temperature. Although some of these variables are typically similar in literature, they can also vary and be optimized for a given electrode. Thus, to obtain the best results for the VACNT IDEs, fluorescent microscopy was used to confirm the amount of fluorescently tagged proteins that were attached to the VACNTs.

It is typically reported that the two-step process is more effective at binding proteins to a surface than the one-step process because the pH can be optimized for each step. In the first step, the VACNT electrode is soaked in both EDC and NHS to activate the carboxyl groups on the surface. Although PBS near neutral pH can be used, the EDC crosslinking is reported as being most efficient at pH 4.5 in buffers without extra carboxyl and amine groups. Thus, MES buffer at pH 4.7 was used for surface activation during step one. This acidic pH is not suitable for proteins, so for the second step, the solution is replaced with PBS at pH 7.4 with the desired streptavidin concentration.

The concentration for EDC and NHS typically vary from 20 mM to 400 mM, with the EDC concentration typically being equivalent or higher than the NHS concentration.

Initial results showed that incubation time in EDC/NHS solution influenced the amount of the streptavidin that was functionalized on the VACNT surface. Under similar conditions, when the activation time was increased from 45 minutes to 90 minutes, the amount of binding improved. Thus, an even longer soaking time of 120 minutes was chosen. The subsequent step of soaking in streptavidin was also a function of time, with longer times increasing the amount of binding. To ensure the best coverage, the electrode was soaked overnight.

The largest observable change in the fluorescent intensity was associated with the concentration of streptavidin during the overnight soaking in PBS. The left images in Figure 3 show the blue fluorescence of IDEs with different streptavidin concentrations, which are listed on the left of the images (20, 100, and 500 μg/mL). It can be seen that the fluorescent streptavidin (blue) was clearly binding to the VACNTs, with both 100 and 500 μg/mL streptavidin showing good intensity. However, the fluorescence at 20 μg/mL streptavidin is hardly visible, suggesting that there may be a minimum threshold concentration to have good coverage on the VACNTs. It should be noted that the
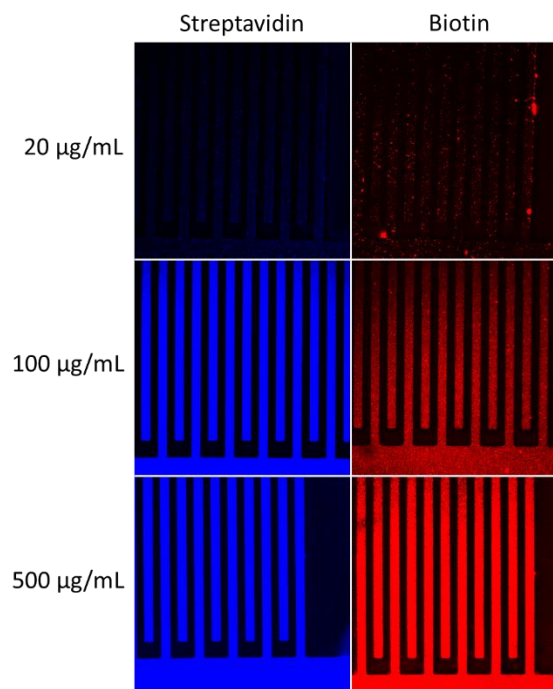

Figure 3. Fluorescent microscopy images confirming fluorescently tagged blue streptavidin and red biotin binding to VACNTs. The concentrations listed (20, 100, 500 μg/mL) are for streptavidin (images shown on the left) and the concentration of biotin (images shown on the right) was constant at 200 μg/mL. The width of fingers and spacing between fingers are both 25 μm.

streptavidin did have some non-specific binding, however, this was not seen in the images because only the top of the VACNT electrodes are in focus on the microscope.

The right images in Figure 3 confirm the binding of fluorescently tagged biotin (red) to the streptavidin on the VACNTs. The concentration of biotin was held constant at 200 µg/mL for each of these devices. Similar to the streptavidin fluorescence, the device with 20 µg/mL streptavidin gave very low intensity biotin fluorescence, except for a few small patch. The biotin results show a greater difference between the 100 and 500 µg/mL streptavidin devices, with 500 µg/mL having a clearly higher intensity. This suggests that although the streptavidin fluorescence looked similar, there was actually a higher loading on the 500 µg/mL device because of the higher biotin fluorescence. Thus, for future tests a concentration of 500 µg/mL streptavidin was used.

Although the fluorescent images give a nice confirmation of binding, the main method of protein detection for this sensor is electrochemical. First, cyclic voltammetry was performed to characterize the VACNT IDEs and to see if any changes were noticeable in the presence of proteins. Figure 4 shows the cyclic voltammograms for one side of the VACNT electrode acting as the working electrode, a platinum wire as the counter electrode and an Ag/AgCl reference electrode with 5 mM ferricyanide and 5 mM ferrocyanide in 0.1 M KCl at a scan rate of 100 mV/s. The bare VACNT curve is compared to the curves of functionalized VACNT electrodes with streptavidin and with both biotin and streptavidin. The overall shape of the curves is very typical of a single electron electrochemical reaction, with anodic and cathodic peaks in current. The peaks are caused by a balance between reaction kinetics and diffusion from the solution. The magnitude of the
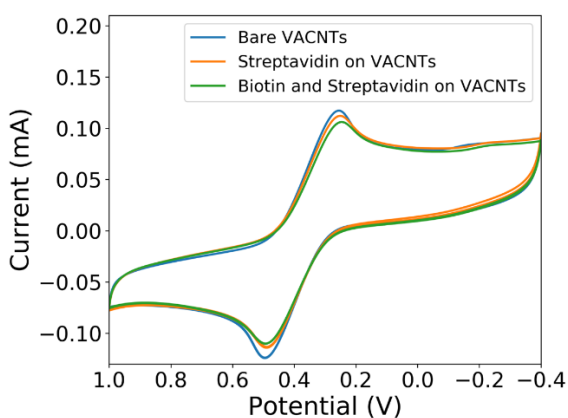

Figure 4. Cyclic voltammograms of bare, streptavidin-coated, and biotin/streptavidin-coated VACNT IDEs with 5 mM ferricyanide and 5 mM ferrocyanide in 0.1 M KCl at a scan rate of 100 mV/s.

current peak i_p can be expressed by the Randles-Sevcik equation:

$$i_p = (2.69\text{x}10^5)n^{3/2}AD^{1/2}Cv^{1/2}$$

where n is the number of electrons (1), A is the area of the electrode (cm^2), D is the diffusion coefficient of ferricyanide ($7.2\text{x}10^{-6}$ cm^2/s), C is the concentration ($5\text{x}10^{-6}$ mol/cm^3), and ν is the scan rate (0.1 V/s). The only variable that is not defined or constrained is the electrode surface area. The exact surface area of the electrode is not known because of the porous and disordered nature of the VACNT electrodes. If the peak current changes it must be due to changes in the electrode surface area. Although the functionalization should have little effect on the geometric surface area, it does influence the electroactive surface area, which is what is being calculated in the Randles-Sevcik equation.

The peak currents in Figure 4 decreased when streptavidin was bound to the VACNTs and then decreased even further when biotin was added to the streptavidin. The peak current of bare CNTs was about 0.120 mA, the streptavidin peak was 0.108 mA, and the biotin/streptavidin peak was 0.102 mA. Thus, the electroactive surface area experienced a total decrease of about 15%.

It should also be noted that the half-wave potential (which closely approximates the formal potential) was about 0.373 V vs Ag/AgCl and the peak-to-peak potential separation was about 240 mV. Both values were slightly higher than expected, with the formal potential of ferricyanide typically being around 0.160 V vs Ag/AgCl and the theoretical peak separation being 59 mV, however this value in real systems is typically reported being closer to 80-100 mV. Many factors may have caused these shifts, but one factor may be the internal resistance within the VACNT electrode along the leads and the fingers of the IDEs.

The second electrochemical test of interest is electrochemical impedance spectroscopy (EIS). During an EIS experiment, a sinusoidal potential is applied to the electrode and the corresponding current is measured to obtain an impedance over a wide range of frequencies. EIS was performed with a two-electrode set up in the same concentration solution used in cyclic voltammetry. The data points in the Nyquist plots in Figure 5A are the measured experimental EIS results for bare, streptavidin-coated, and biotin/streptavidin-coated VACNTs, where real impedance (Z') is on the x-axis and imaginary impedance (-Z") is on the y-axis. While the overall changes in the spectrum may appear to be small when the VACNTs are bound with proteins, the inset in Figure 5A shows that in between the two partial semi-circles there is a significant change in the imaginary impedance.
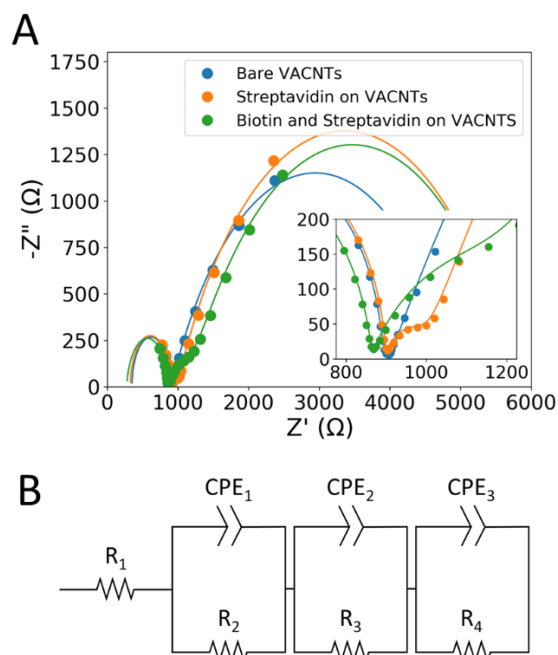
Figure 5. (A) Experimental (circles) and simulated (lines) Nyquist plots of bare, streptavidin-coated, and biotin/streptavidin-coated VACNT IDEs. The x-axis is the real impedance and the y-axis is the imaginary impedance. Inset: Zoomed in view showing large change in imaginary impedance in between larger semi-circles. (B) Equivalent circuit used to model the impedance change of the VACNT sensor.

The EIS data can be represented by an equivalent electrical circuit as shown in Figure 5B. Each semi-circular shape in the Nyquist plot is representative of a resistance-capacitor time constant. The bare VACNT could be described with just two time constants, but the functionalization brings the beginning of another semi-circle. Thus, three time constants are used to describe the biosensor. The equivalent circuit uses constant phase elements (CPEs) in place of capacitors because the semi-circles are depressed, which is more apparent when the x-axis and y-axis have the same scale. The resistance R_1 and the first time constant (CPE_1/R_2) are representative of the internal resistance and capacitance within the sensor. This is known because a shorted device, caused by IDE fingers touching, was tested without soaking in ferricyanide solution and gave nearly the same curve as the initial part of the original EIS results. The second time constant (CPE_2/R_3) is caused by the binding events occurring at the VACNT surface. The final time constant (CPE_3/R_4) is representative of the ferricyanide kinetics at the VACNT electrode surface.

With an equivalent circuit, experimental EIS data can be curve fit to determine the values of the circuit elements. The data was curve fit using open source software (EIS Spectrum Analyzer) and then the simulated results were plotted as the solid lines in Figure 5A. The simulated results matched the experimental results with reasonable accuracy. Table 1 gives a summary of the variables for the bare and functionalized VACNT IDEs. Note that in the table the variables P and n are related to the impedance of the CPE by the following relation:

$$Z_{CPE} = \frac{1}{P(\omega i)^n}$$

Table 1. Values of circuit elements of curve fit EIS experimental data.

Element	Bare	Streptavidin	Biotin
R_1	351	326	277
R_2	533	571	585
R_3	24.9	96.2	341
R_4	4073	4744	4554
P_1	4.70e-10	6.13e-10	1.12e-9
n_1	1.00	0.978	0.927
P_2	3.80e-5	3.86e-5	1.07e-4
n_2	0.635	0.755	0.644
P_3	0.000516	0.000563	0.000605
n_3	0.655	0.670	0.660

The largest change from streptavidin and biotin is manifest in the resistance R_3. Starting at 24.9 Ω, R_3 increases to 96.2 Ω with streptavidin and then 341 Ω with biotin and streptavidin. This represents an increase of about 14 times, which is much larger than the change associated with cyclic voltammetry. Monitoring this resistance change would thus provide an effective path for detection of binding events at the VACNT surface, which could be used to determine concentrations of target analyte. With such a large change manifest, it is likely that this would correlate with concentration of biotin and move toward creating a point-of-care electrochemical biosensor.

CONCLUSION

The VACNT IDEs have been shown to be effective biosensors by taking advantage of high protein loading on the VACNT surfaces. This is an important step in creating effective point-of-care biosensors. Fluorescence intensity was used to find the best binding conditions for the VACNT electrode, which binding was then measured by cyclic voltammetry and electrochemical impedance spectroscopy. The change in imaginary impedance was significant when adding streptavidin by itself and then even larger when adding biotin to the streptavidin. The unique change in impedance for the representative target analyte bound

to the VACNT electrode surface could be used to detect a large range of target analyte depending on what is first functionalized to the VACNT surface. Thus, future work could involve investigating other target analyte and measuring the change in imaginary impedance as a function of analyte concentration.

REFERENCES

[1] S.A. Zaidi, J.H. Shin, Recent Developments in Nanostructure Based Electrochemical Glucose Sensors, Talanta 149 (2016) 30-42.

[2] M. Varshney, Y. Li, B. Srinivasan, S. Tung, A label-free, microfluidics and interdigitated array microelectrode-based impedance biosensor in combination with nanoparticles immunoseparation for detection of Escherichia coli O157:H7 in food samples, Sensors and Actuators B: Chemical 128(1) (2007) 99-107.

[3] K. Dhara, D.R. Mahapatra, Electrochemical Nonenzymatic Sensing of Glucose Using Advanced Nanomaterials, Microchimica Acta 185(1) (2018) 49.

[4] F. Schröper, D. Brüggemann, Y. Mourzina, B. Wolfrum, A. Offenhäusser, D. Mayer, Analyzing the electroactive surface of gold nanopillars by electrochemical methods for electrode miniaturization, Electrochimica Acta 53(21) (2008) 6265-6272.

[5] S. Ding, S.R. Das, B.J. Brownlee, K. Parate, T.M. Davis, L.R. Stromberg, E.K.L. Chan, J. Katz, B.D. Iverson, J.C. Claussen, CIP2A Immunosensor Comprised of Vertically-aligned Carbon Nanotube Interdigitated Electrodes Towards Point-of-Care Oral Cancer Screening, Biosensors and Bioelectronics 117 (2018) 68-74.

[6] B.J. Brownlee, K.M. Marr, J.C. Claussen, B.D. Iverson, Improving Sensitivity of Electrochemical Sensors with Convective Transport in Free-standing, Carbon Nanotube Structures, Sensors and Actuators B: Chemical 246 (2017) 20-28.

[7] D. Kim, A.E. Herr, Protein immobilization techniques for microfluidic assays, Biomicrofluidics 7(4) (2013) 041501.

[8] K.M. Marr, B. Chen, E.J. Mootz, J. Geder, M. Pruessner, B.J. Melde, R.R. Vanfleet, I.L. Medintz, B.D. Iverson, J.C. Claussen, High Aspect Ratio Carbon Nanotube Membranes Decorated with Pt Nanoparticle Urchins for Micro Underwater Vehicle Propulsion via H2O2 Decomposition, ACS Nano 9(8) (2015) 7791-7803.